Adsorbed Proteins Influence the Biological Activity and Molecular Targeting of Nanomaterials

Debamitra Dutta,* Shanmugavelayutham Kamakshi Sundaram,† Justin Gary Teeguarden,‡ Brian Joseph Riley,†
Leonard Sheldon Fifield,† Jon Morrell Jacobs,§
Shane Raymond Addleman,¶ George Alan Kaysen,‖ Brij Mohan Moudgil,* and Thomas Joseph Weber‖‖‖,[1]

*Particle Engineering Research Center and the Department of Materials Science and Engineering, University of Florida, Gainesville, Florida 32611;
†Advanced Processing and Applications Group; ‡Biological Monitoring and Modeling; §Process Science and Engineering, Environmental
Technology Directorate; ¶Biological Systems Analysis and Mass Spectrometry, Pacific Northwest National Laboratory, Richland, Washington 99354;
‖Division of Nephrology, Department of Medicine and the Department of Biochemistry and Molecular Medicine, University of California, Davis,
California 95616, and the Department of Veteran's Affairs, Northern California Health Care System, Mather, California 95655; and ‖‖‖Cell Biology
and Biochemistry, Biological Sciences Division, Pacific Northwest National Laboratory, Richland, Washington 99354

The possible combination of specific physicochemical properties operating at unique sites of action within cells and tissues has led to considerable uncertainty surrounding nanomaterial toxic potential. We have investigated the importance of proteins adsorbed onto the surface of two distinct classes of nanomaterials (single-walled carbon nanotubes [SWCNTs]; 10-nm amorphous silica) in guiding nanomaterial uptake or toxicity in the RAW 264.7 macrophage–like model. Albumin was identified as the major fetal bovine or human serum/plasma protein adsorbed onto SWCNTs, while a distinct protein adsorption profile was observed when plasma from the Nagase analbuminemic rat was used. Damaged or structurally altered albumin is rapidly cleared from systemic circulation by scavenger receptors. We observed that SWCNTs inhibited the induction of cyclooxygenase-2 (Cox-2) by lipopolysaccharide (LPS; 1 ng/ml, 6 h) and this anti-inflammatory response was inhibited by fucoidan (scavenger receptor antagonist). Fucoidan also reduced the uptake of fluorescent SWCNTs (Alexa$_{647}$). Precoating SWCNTs with a nonionic surfactant (Pluronic F127) inhibited albumin adsorption and anti-inflammatory properties. Albumin-coated SWCNTs reduced LPS-mediated Cox-2 induction under serum-free conditions. SWCNTs did not reduce binding of LPS$_{Alexa488}$ to RAW 264.7 cells. The profile of proteins adsorbed onto amorphous silica particles (50–1000 nm) was qualitatively different, relative to SWCNTs, and precoating amorphous silica with Pluronic F127 dramatically reduced the adsorption of serum proteins and toxicity. Collectively, these observations suggest an important role for adsorbed proteins in modulating the uptake and toxicity of SWCNTs and nano-sized amorphous silica.

Key Words: scavenger receptor; albumin; carbon nanotube; inflammation.

[1] To whom correspondence should be addressed at the Department of Cell Biology and Biochemistry, Pacific Northwest National Laboratory, 790 6th Street, P7-56, Richland, WA 99354. Fax: (509) 376-6767. E-mail: thomas. weber@pnl.gov.

Nanomaterials are typically defined as engineered structures with at least one dimension of 100 nm or less, though from the perspective of biology this definition may be too narrow (Teeguarden *et al.,* 2007). Nanomaterials can have unique physicochemical properties that result from the combination of their small size, chemical composition, surface structure, solubility, shape, and aggregation (Nel *et al.,* 2006). Engineered nanomaterials also take on a variety of shapes including spheres, fibers, tubes, and rings. Intentional modification of nanomaterial physicochemical properties results in unique characteristics, including high conductivity, strength, durability, and chemical reactivity that are finding applications in many fields. Importantly, materials that are inert in bulk form may be toxic in nano-sized form (Nel *et al.,* 2006; Oberdorster *et al.,* 2005 and references therein), arguing that all nanomaterials must be systematically evaluated for their toxic potential. Rapid growth in the number of nanostructured materials available and the increasing number of apparent applications of nanotechnology make the toxicological issues associated with these new materials of escalating significance. However, there is uncertainty surrounding human health issues and environmental effects of these poorly characterized materials. Nano-sized particles can cross cellular membranes by nonphagocytic mechanisms (Geiser *et al.,* 2005), which may facilitate their access to sites within cells and tissues not previously or routinely encountered, further contributing to uncertainty surrounding their toxic potential.

While significant emphasis has been placed on size- and physicochemical property–dependent toxicity of nanomaterials, less emphasis has been placed on approaches to predict nanomaterial disposition, which in turn is frequently a determinant of toxicity. Size is a limiting factor in visualizing the tissue and subcellular localization of nanomaterials, making accurate assessment of nanomaterial disposition challenging (Mercer *et al.,* 2007). In this context, proteins adsorbed to the surface of particles, liposomes, toxicants, and a variety of drug delivery

agents often play a decisive role in governing disposition (Douglas *et al.*, 1987; Goppert and Muller, 2005; Moghimi *et al.*, 1993). Opsonins have long been associated with the rapid uptake of particles by the mononuclear phagocytic system (Douglas *et al.*, 1987). Surfactants or coatings that repel protein adsorption have been developed to circumvent the limitations associated with the mononuclear phagocytic system in drug targeting and illustrate the importance of adsorbed proteins in guiding disposition. As one example, the disposition of polystyrene nanospheres and colloidal gold nanoparticles with and without poloxamine-908 coating have been examined (Moghimi *et al.*, 1993). Uncoated nanospheres formed a complex with fibronectin and were primarily taken up by hepatic Kupffer cells. Poloxamine-908 coating dramatically reduced fibronectin adsorption and liver accumulation. As a second example, polysorbate 80–coated polybutylcyanoacrylate (PBCA) nanoparticles are under investigation for drug delivery to the brain (Goppert and Muller, 2005). The polysorbate coating results in the preferential adsorption of apolipoprotein E (apoE), which in turn, appears to be an important determinant for passage through the blood-brain barrier. Surfactants that did not promote apoE adsorption did not promote passage through the blood-brain barrier, and coating PBCA particles with apoE in the absence of coating with polysorbate 80 resulted in efficient delivery of the particles to the brain.

We hypothesize that proteins adsorbed onto nanomaterials will play an important role in directing their disposition and toxicity. If our hypothesis is correct, then defining the stoichiometry of proteins adsorbed onto nanomaterials *a priori* will provide important clues regarding sites of uptake for consideration in initial toxicological investigations. To test this hypothesis, we have investigated the toxicity of two elementally (i.e., carbon vs. silica) distinct classes of nanomaterials with tubular (single-walled carbon nanotubes [SWCNTs]) or spherical (10-nm amorphous silica) structures with and without surfactant coating to prevent the adsorption of serum proteins. The fundamental differences between these nanomaterials are expected to result in distinct protein adsorption profiles due to their discrete physicochemical properties as well as induce toxicity by different modes of action. These differences will provide a reasonable initial evaluation of the relative importance of adsorbed proteins in guiding the toxicity of nanomaterials. We observe that resuspension of nanomaterials in Pluronic F127 dramatically reduces protein adsorption and toxic potential of both SWCNTs and 10-nm amorphous silica. In addition, adsorption of albumin onto SWCNTs appears to target the SWCNT-albumin complex to scavenger receptors. Collectively, our data suggest that careful attention to protein adsorption profiles can contribute to nanomaterial toxicity assessment.

MATERIALS AND METHODS

Materials

RPMI 1640 medium, sodium pyruvate, fetal bovine serum (FBS), L-glutamine, penicillin, streptomycin, Pluronic F127, and Alexa$_{488}$-labeled

bacterial lipopolysaccharide (LPS$_{Alexa488}$) were purchased from Invitrogen (Carlsbad, CA). LPS from *Escherichia coli* strain O127:B8 was purchased from Sigma-Aldrich Chemical (lot number 31K4120, 600,000 EU/mg protein; St Louis, MO). Human serum was purchased from Golden West Biologicals (Temecula, CA). Nagase analbuminemic rat (NAR) plasma was supplied by Dr George Kaysen (UC-Davis, CA). Anti-albumin and glyceraldehyde 3-phosphate dehydrogenase (GAPDH) antibodies were from Abcam (Cambridge, MA). Anti-cyclooxygenase-2 (Cox-2) antibody was from Cayman Chemical (Ann Arbor, MI). Anti-inducible nitric oxide synthase (iNOS) and actin antibodies were from Santa Cruz Biotechnology, Inc. (Santa Cruz, CA). SWCNTs (Carbolex AP-grade) were from Sigma-Aldrich. The 10-nm amorphous silica suspension was from Polysciences, Inc. (Warrington, PA).

Cell Culture

The RAW 264.7 murine macrophage cell line was obtained from the American Type Culture Collection (Rockville, MD). Cells were maintained in RPMI 1640 supplemented with 10% FBS, 2mM L-glutamine, 1mM sodium pyruvate, 100 units/ml penicillin, and 0.1 mg/ml streptomycin in a humidified atmosphere of 5% CO_2 and 95% air at 37°C. Cells were subcultured using a rubber blade cell scraper (Sarstedt, Newton, NC).

Particle Characterization

Surface area. The gas adsorption technique Brunauer-Emmett-Teller (BET)-specific surface area analysis was used to determine the surface area of nonfunctionalized as-received (Sigma-Aldrich) SWCNTs in the dry state. To remove any physisorbed species from the surface, dry carbon nanotubes were degassed at elevated temperature (212 K) under vacuum for 24 h before performing surface area measurements using N_2 gas adsorption (77 K) onto the SWCNTs.

Transmission electron microscopy. High-resolution transmission electron microscopy (TEM) imaging was performed using JEOL TEM 2010F HRTEM. TEM samples were prepared by placing a drop of solution prepared by dispersing SWCNTs in denatured ethanol directly on a lacey carbon grid (200 mesh), and imaging was done at 200 kV.

Scanning electron microscope-Energy dispersive spectrometry. Nonfunctionalized as-received SWCNTs were studied on a scanning electron microscope (SEM JEOL-6100) in energy dispersive spectrometry (EDS) mode to detect the compositional elements present in the carbon nanotube sample. Aluminum stubs were smeared with silver paint and SWCNTs in the dry state placed on the stubs and attached to copper tapes to make them conductive. The metallic stubs were then placed on the holder and introduced into the instrument at 10 kV.

Zeta potential. Brookhaven ZetaPlus (Brookhaven Instruments Corporation, Holtsville, NY) was used to determine the surface charge on the amorphous silica nanoparticles as dispersed in each of the different experimental conditions used for this study: ultrapure water, normal growth medium, and Pluronic F127 + normal growth medium. The pH of the sample solutions was monitored using a standard laboratory pH meter, and all readings were conducted at room temperature.

Particle size measurements. Dynamic light scattering spectroscopy (Nanotrak Particle Size Analyser—Microtrac Inc., Montgomeryville, PA 18936) was used to determine the surface charge on the 10-nm amorphous silica nanoparticles as dispersed in each of the different experimental conditions used for this study: ultrapure water, normal growth medium, and Pluronic F127 + normal growth medium.

Nanomaterial Resuspension and In Vitro Exposure

SWCNTs were added directly to a sterile 15 ml conical in a Mettler Toledo AB104 scale using an autoclaved spatula until approximately 5–10 mg (dry weight) had been added. The 15 ml conical was then immediately capped, transported to a tissue culture hood, and normal growth medium (containing 10% FBS and supplements described above) was added to produce a final concentration of 1 mg SWCNTs/ml medium. SWCNTs were then resuspended

by sonication in a Branson Tabletop Ultrasonic Cleaner (Model 1510) for 20 min at room temperature with vortexing at 5 min intervals. An equal volume of normal growth medium was pipetted into a 15-ml conical and sonicated in parallel for use as a "sonicated medium" control. The SWCNT suspension was inverted several times prior to removal of an aliquot for dilution in normal growth medium to the concentrations indicated. As a control, an equal volume of sonicated medium was added to normal growth medium to account for the contributions of sonicated medium components in the cellular response to SWCNTs. Under these conditions, the 15 ml conical could be maintained for several weeks on a benchtop and the medium remained black, suggesting that a significant portion of the SWCNTs did not appreciably settle by gravity. However, an undefined fraction of the SWCNTs could be observed to settle by gravity, as evidenced by the formation of a small pellet at the bottom of the 15 ml conical, indicating that cells were likely exposed to a mixture of dispersed and aggregated SWCNTs.

Qualitative Protein Adsorption Profiles

Nanomaterials were resuspended in normal growth medium containing 10% FBS by sonication for 20 min. Proteins adsorbed onto nanomaterials that sediment at $5000 \times g$ (5 min) were collected and washed three times by resuspension in PBS with vortexing, followed by centrifugation and aspiration of the supernatant. For amorphous silica, centrifugation resulted in a fraction of the sedimented silica to aggregate so extensively as to not be disrupted during the washing stages. To minimize the potential contribution of nonadsorbed serum proteins trapped within these aggregates to the protein adsorption profiles, samples were allowed to gravity settle for approximately 2 min, the supernatant was transferred to new tubes (the aggregates were discarded), and the supernatant was processed as described above. Therefore, the protein adsorption profiles are qualitative, and protein loading was adjusted between groups to enable evaluation of the protein adsorption profiles under comparable protein loads. Proteins were desorbed from nanomaterials by sonication in Laemli loading buffer for 20 min followed by incubation in boiling water for 5 min. The samples were then subjected to a final centrifugation step ($18,000 \times g$ for 5 min) to sediment aggregates of nanomaterials that were visible, and the supernatant was analyzed by sodium dodecyl sulfate-polyacrylamide gel electrophoresis (SDS-PAGE). Separated proteins were detected by Coomassie Blue staining and SYPRO Ruby protein gel stain. In some experiments, nanomaterials were resuspended in Pluronic F127 by sonication for 20 min followed by incubation with FBS (final concentration of 10%) for 60 min with gentle agitation. Proteins adsorbed to nanomaterials coated with Pluronic F127 were then processed as described above.

Cytotoxicity Determination by Cell Counts

Randomly cycling preconfluent RAW 264.7 cells (seeded in 35 mm dishes) were exposed to SWCNTs or amorphous silica (resuspended as described above) at the concentrations and times indicated in the Figure legends. Following exposure to nanomaterials, medium was aspirated, 1 ml of PBS was added to each dish, and cells were harvested from the dishes using a rubber blade cell scraper (Sarstedt, Newton, NC). Cell number was quantified using a Coulter Counter.

Mass Spectrometry Analysis

Proteins adsorbed onto Pluronic F127–coated SWCNTs were resolved by SDS-PAGE, and selected bands were cut from the gel for identification by mass spectrometry (MS). The digested gel band was analyzed via liquid chromatography (LC)-tandem MS (MS/MS) using a previously described (Shen *et al.,* 2001) reversed-phase capillary liquid chromatography system coupled to a Finnigan LTQ ion trap mass spectrometer (ThermoFinnigan, San Jose, CA). The LC-MS/MS data analysis was performed using SEQUEST analysis software to match the MS/MS fragmentation spectra with sequences from the March 2006 National Center for Biotechnology Information *Bos taurus* database, containing 33,543 entries. The criteria selected for filtering followed methods based upon a reverse database false positive model which has been shown to give ~95% confidence for an entire protein dataset (Qian *et al.,* 2005).

SWCNT Labeling with Alexa 647

SWCNTs were oxidized in strong acid and peroxide to create carboxylic acid functionality on their surface (Zhao *et al.,* 2002). The acid groups on the SWCNTs were then coupled with an amine-terminated fluorescent dye using standard protein cross-linking chemistry (Hermanson, 1996). Details of the steps used are as follows: concentrated sulfuric acid (H_2SO_4) was slowly added to 30% hydrogen peroxide (H_2O_2) to form a 3:1 volume ratio solution. SWCNTs were stirred into a 3:1 (vol/vol) solution of concentrated H_2SO_4 and 30% H_2O_2 at a concentration of approximately 2 mg of SWCNTs per mg of solution. The mixture was sonicated in a bath ultrasonic cleaner (Branson 1510) for 1 min and then removed from the bath and stirred for 10 min. This sonication/stir cycle was repeated two more times. The resulting black solution was filtered through a polytetrafluoroethylene (PTFE) filter membrane (0.45 μm pore), being careful not to filter the SWCNTs to dryness. The wet SWCNT deposit was then rinsed with deionized (DI) water (approximately 20 times the volume of the acid/peroxide solution) until the pH of the filtrate matched that of the DI water used. The oxidized SWCNTs (CNT-COOH) were recovered by sonicating the still-wet SWCNT/PTFE membrane in DI water (which became black). The SWCNT-COOH solution was centrifuged (Fisher Scientific accuSpin400) at 5000 rpm for 10 min. The supernatant was removed and centrifuged at 10,000 rpm for 20 min. Aggregates visible after allowing the solution to sit overnight were removed by centrifugation to produce a stable aqueous suspension with approximate concentration of 0.5 mg SWCNT-COOH per 1 ml solution. 1-Ethyl-3-(3-dimethylaminopropyl) carbodiimide hydrochloride (EDC; Sigma-Aldrich), N-hydroxysulfosuccinimide (S-NHS, sodium salt; Molecular Probes, Eugene, OR), and NA647 (Alexa Fluor 647 cadaverine, disodium salt; Molecular Probes) were each dissolved in DI water and added to the SWCNT-COOH aqueous solution, diluted to be approximately 0.25 mg SWCNT-COOH per ml water. The molar concentration of NA647 and EDC used were approximately equivalent and in large (> 10 times) excess to the acid groups present on the SWCNTs. S-NHS was used in large excess. The combined solution was stirred at room temperature for 2 h. The solution was then filtered through a Polyvinylidene Difluoride membrane (0.2 μm pore) and rinsed repeatedly with water to remove the excess reagents. The SWCNTs were recovered by sonicating the membrane in fresh DI water and depositing onto a new membrane, which was again rinsed with DI water. The deposit was filtered to dryness, and the dye-functionalized SWCNTs were recovered as a solid from the membrane.

Measurement of Cox-2 and iNOS Expression

Cox-2 and iNOS expression were quantified by Western blot analysis according to our published methods (Weber *et al.,* 2006). Titers used were actin (1:3000), albumin (1:3000), Cox-2 (1:3000), GAPDH (1:10,000), and iNOS (1:3000). All secondary antibodies were used at a dilution of 1:4000. Detection and quantification of Cox-2 and iNOS bands was accomplished using the Pierce SuperSignal WestFemto chemiluminescent substrate and a LumiImager (Roche Diagnostics, Mannheim, Germany), respectively.

Estimation of SWCNT Concentration In Suspension Following Sonication

In Figure 10, we investigated the anti-inflammatory properties associated with SWCNTs coated with albumin. In this experiment, large SWCNT aggregates were allowed to settle by gravity for 1 h, and the supernatant was used at increasing volumes in the experimental design. To estimate the concentration of SWCNTs remaining in suspension, we constructed a standard curve using the crude SWCNT suspension (aggregates and SWCNTs remaining in suspension) since this represents a known concentration based on the initial mass of SWCNTs used to construct the standard curve. The concentration of SWCNTs remaining in suspension was then extrapolated from this standard curve (determined at an absorbance wavelength of 405 nm). Linear regression analysis indicated that ABS_{450} value highly correlated with SWCNT concentration under these conditions ($r^2 \geq 0.99$; data not shown). This approach was used to provide an estimate of SWCNT concentration remaining in suspension rather than simply reporting the volume of supernatant used which was deemed uninformative. For experiments addressing albumin-

opsinized SWCNTs, cells were maintained and treated with nanotubes in RPMI 1640 supplemented with 100 µg/ml bovine serum albumin (BSA), 2mM L-glutamine, 1mM sodium pyruvate, 100 units/ml penicillin, and 0.1 mg/ml streptomycin.

Statistics

Individual comparisons were made using the Students *t*-test or ANOVA with a *post hoc* Student's Newman-Keul test, as appropriate. The $p < 0.05$ level was accepted as significant.

RESULTS

We have chosen to investigate the relative importance of adsorbed proteins in guiding nanomaterial toxicity using two structurally distinct classes of nanomaterials, namely SWCNTs and 10-nm amorphous silica. Nanomaterial characteristics that have been determined are illustrated below. In some experiments, the nonionic surfactant Pluronic F127 was used to coat nanomaterials to improve dispersion while reducing protein adsorption. Pluronic F127 is a difunctional block copolymer surfactant terminating in primary hydroxyl groups that is generally nontoxic. We have not observed any evidence of toxicity in Pluronic F127–treated cells at concentrations at least 100-fold higher than used in the present studies (data not shown).

SWCNT Particle Characteristics

The majority of our studies have focused on SWCNTs resuspended in normal growth medium. However, crystallization of salts and other components of the normal growth medium obscured the resolution of SWCNT particle characterized by TEM under these conditions (data not shown). TEM analysis of the SWCNTs in ethanol and water revealed long ropes of nanotubes aligned in parallel and what appeared to be bundles of material (Fig. 1). At lower magnification, it was clear the ropes of nanotubes were > 150-nm long (data not shown). The measured BET of the as-received SWCNTs was 274.1 m^2/g; however, the surface area may be different in solution, particularly in experiments using albumin as opsin where SWCNTs were allowed to flocculate and settle before administration to cells. SEM-EDS analysis of the carbon nanotubes showed the presence of silica, yttrium, and nickel at 0.12, 2.9, and 17.29% by weight, respectively. SWCNTs of (2.74 cm^2/µg SWCNT) can be used to convert data from mass to surface area for these experiments.

Amorphous Silica Particle Characteristics

The nominal particle size of the 10-nm amorphous silica from PolySciences was verified using TEM (Fig. 2). TEM images showed agglomerates of particles with a primary particle size near 10 nm as reported by the manufacturer. To verify that agglomeration is an artifact of the drying process required for TEM, particle size was verified in water and the two treatments used in experiments, namely coating with
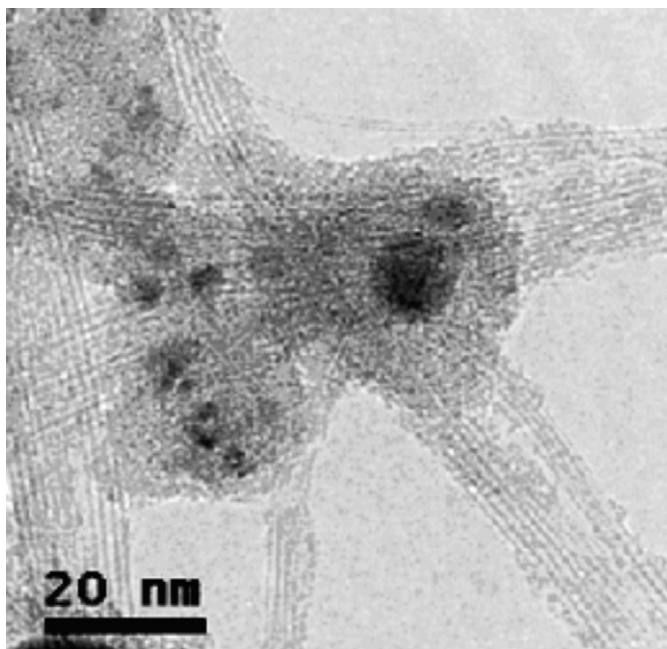

FIG. 1. TEM analysis of SWCNTs. TEM samples were prepared as described in ''Materials and Methods'' section and imaged at 200 kV. The data suggest that the SWCNTs exist as a mixture of clumps, ropes, and bundles under these conditions.

Pluronic F127/resuspension in normal growth media and resuspension in normal growth medium alone. In water, the number average primary particle size was 11.1 nm. In pluronic plus normal growth media, the average primary particle size was 12.3 nm, and the average primary particle size increased to 27.2 nm when resuspended in normal growth medium alone (Fig. 3). Thus, there appeared to be very modest agglomeration when 10-nm amorphous silica was resuspended in normal growth medium alone. The mean zeta potential (SE) of silica (at 25°C) was − 65.9 mV (1.59), − 4.8 mV (3.0), and − 37.2 (4.18) in water (pH 5.5), normal growth media (pH 7.4), and pluronic + normal growth media (pH 7.4), respectively. The two concentrations of 10-nm amorphous silica used in the present studies can be converted to surface area or particle number based on the following: 0.78 µg/ml 10-nm amorphous silica = 2.12 cm^2/ml = 6.77×10^{11} particles/ml and 1.66 µg/ml 10-nm amorphous silica = 4.53 cm^2/ml = 1.44×10^{12} particles/ml.

Identification of Serum Proteins Adsorbed onto SWCNTs

We examined (qualitatively) proteins adsorbed onto two preparations of SWCNTs, namely (1) SWCNTs resuspended in normal growth medium supplemented with 10% FBS by sonication and (2) SWCNTs resuspended in Pluronic F127 by sonication followed by incubation with FBS (10% final concentration) for 60 min with gentle rocking. Proteins were desorbed from SWCNTs as described in ''Materials and
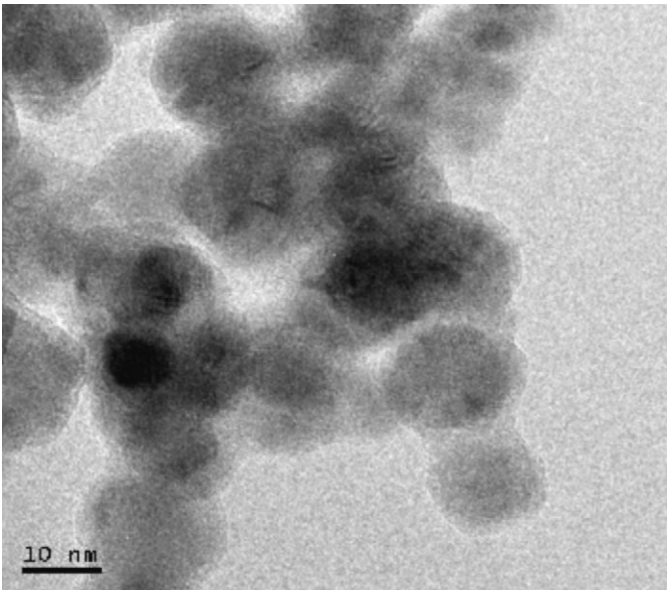
FIG. 2. TEM analysis of 10-nm amorphous silica. TEM samples were prepared as described in ''Materials and Methods'' section and imaged at 200 kV.

Methods'' section, separated by SDS-PAGE and detected using SYPRO Ruby protein gel stain. Distinct protein adsorption profiles were observed when SWCNTs were resuspended in normal growth medium versus emulsifying agent (Pluronic F127) prior to incubation with normal growth medium (Fig. 4). Resuspension in normal growth medium was associated with a major band in the 49- to 62-kDa range of the gel along with several additional but less abundant proteins. This band was the dominant protein adsorbed to SWCNTs whether they were passively incubated with FBS or were resuspended by sonication (data not shown). The major band appearing in the 49- to 62-kDa range was not detected in preparations where SWCNTs were resuspended in Pluronic F127 prior to
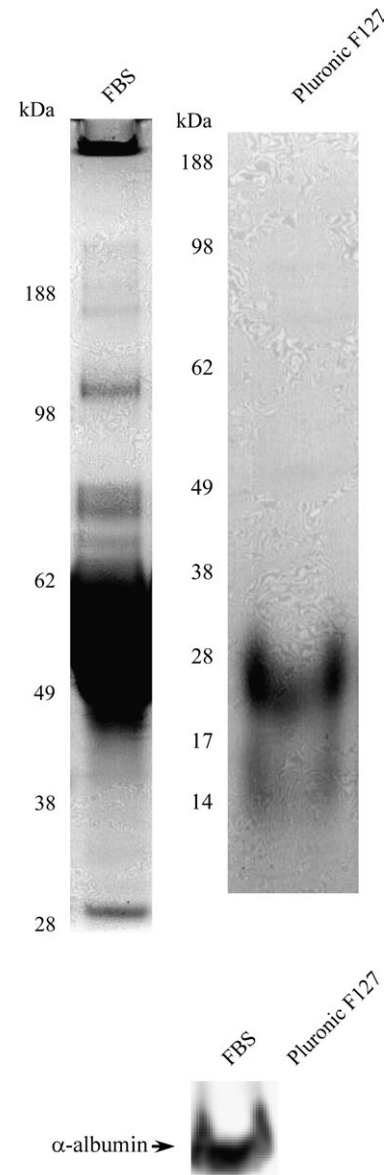

FIG. 4. Adsorption of FBS proteins to SWCNTs with or without Pluronic F127 coating. SWCNTs were resuspended in normal growth medium by sonication or Pluronic F127 by sonication followed by incubation with FBS (10% final) for 60 min as described in ''Materials and Methods'' section. SWCNTs were then washed three times with PBS, proteins desorbed, and analyzed by SDS-PAGE and anti-albumin Western blot. Similar results were observed in five separate experiments.

FIG. 3. Estimation of amorphous silica aggregation states. Amorphous silica was resuspended in water (cross), Pluronic F127 (solid circle), or normal growth medium (solid square), and average particle diameter was determined as described in ''Materials and Methods'' section.

incubation with FBS and was subsequently identified as albumin by Western blot analysis (Fig. 4). A similar protein adsorption profile was observed when SWCNTs were resuspended in undiluted FBS versus normal growth medium (10% FBS; data not shown). The serum proteins adsorbed to Pluronic F127–coated SWCNTs (14–28 kDa range) were excised from the gel, subjected to in-gel tryptic digestion, analyzed by tandem MS as described in "Materials and Methods" section, and identified from a subsequent search

against the *B. taurus* database. Proteins predominantly detected by MS with predicted molecular weights in the 14- to 28-kDa range included casein alpha-S1, casein beta, casein kappa, hemoglobin beta, hemoglobin gamma, and lactoglobulin beta. Additional proteins that were detected with multiple unique peptides, but were inconsistent with the 14- to 28-kDa range of the gel, included alpha-2-HS-glycoprotein, apoplipoprotein A-II, keratin 10, and keratin 15. Such identifications are likely due to the sensitivity of the MS coupled with identification of protein fragments of these higher abundant bovine serum proteins in this mass range. From these results, casein-related proteins were the strongest candidates for the proteins adsorbed to SWCNTs resuspended in emulsifying agent in the 14- to 28-kDa range, and we confirmed that purified casein adsorbs onto SWCNTs coated with Pluronic F127 (data not shown).

Identification of Protein Adsorption Profiles Associated with SWCNTs Resuspended in NAR or Human Serum/Plasma

We next examined protein adsorption profiles associated with SWCNTs resuspended in plasma from NAR versus human serum and plasma (Fig. 5). The protein adsorption profile associated with albumin-deficient NAR plasma (from four individual animals) was significantly different from the protein adsorption profile associated with human serum/plasma and FBS (compare Figs. 4 and 5). Albumin appeared to be the prominent protein adsorbed to SWCNTs resuspended in human serum and plasma as confirmed by Western blot analysis (Fig. 5, bottom). Within the limits of detection, the protein adsorption profile associated with human serum versus plasma was comparable. Collectively, our data suggest that albumin is the major protein adsorbed onto SWCNTs from plasma and serum fractions and that resuspending SWCNTs in emulsifying agent significantly alters the protein adsorption profile.

SWCNT Toxicity Assessment by Measurements of Cell Proliferation

As an initial range finding study for toxicological investigations, we determined whether SWCNTS inhibited cell proliferation as a sensitive index of toxicity. RAW 264.7 cells were treated with SWCNTs (12.5–25 μg/ml nominal medium concentration; dispersed in normal growth medium) for 24 h, and cell number was determined using a Coulter Counter as described in "Materials and Methods" section. SWCNTs induced a marginal but dose-dependent inhibition of proliferation, relative to controls treated with an equal volume of sonicated medium (Fig. 6). Thus, at the concentration used for the present studies, SWCNTs induce limited toxicity, as determined by measurements of cell proliferation. This observation is in contrast to 10-nm amorphous silica particles that induce a marked decrease in cell proliferation under these conditions (illustrated in figure 13 below) suggesting different modes of action for these nanomaterial preparations.
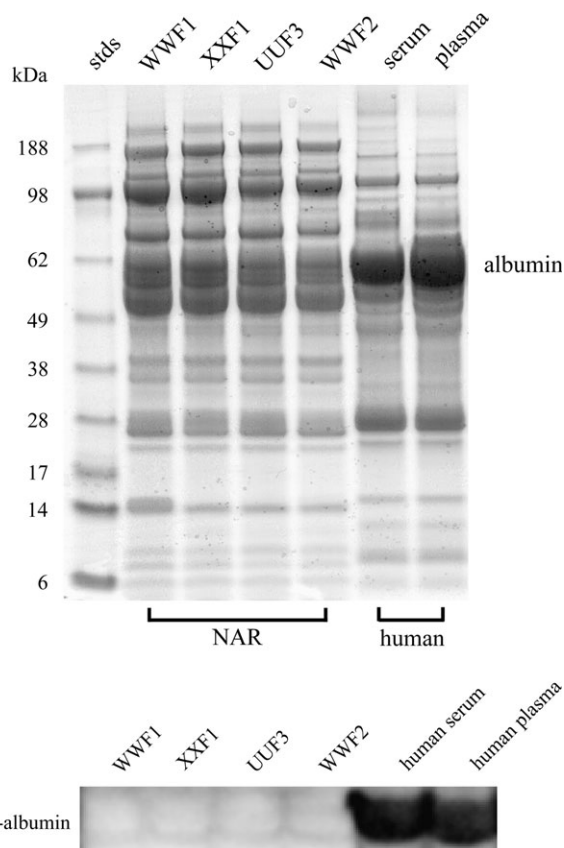

FIG. 5. Protein adsorption profile associated with SWCNTs incubated with NAR plasma, human plasma, or human serum. SWCNTs were resuspended in NAR or human plasma/serum (10% final in RPMI) by sonication as described in "Materials and Methods" section. SWCNTs were then washed three times with PBS, proteins desorbed, and analyzed by SDS-PAGE and anti-albumin Western blot. Similar results were observed in three separate experiments.

SWCNT Effects on the Inflammatory Response to Endotoxin in RAW 264.7 Cells

Cox-2 and iNOS, used as biomarkers of the inflammatory response, were not induced by SWCNTs alone (at concentrations up to 50 μg/ml; 6 and 24 h time points; data not shown). We next examined whether SWCNTs modulated the inflammatory response to LPS, and our results are summarized in Figure 7. Treatment of RAW 264.7 cells with LPS for 6 h resulted in a significant increase in Cox-2 expression. Cox-2 induction by LPS was inhibited by cotreatment with SWCNTs but not sonicated medium used as control (diluted 1:100 to account for sonicated medium effects associated with the highest concentration of SWCNTs investigated). Interestingly, the inhibition of LPS-mediated Cox-2 induction by SWCNTs was reversed by fucoidan (25 μg/ml), which is reported to be a class A scavenger receptor antagonist (Krieger and Herz, 1994). Collectively, these results suggest that the anti-inflammatory effects of SWCNTs resuspended in FBS are mediated by scavenger receptors.
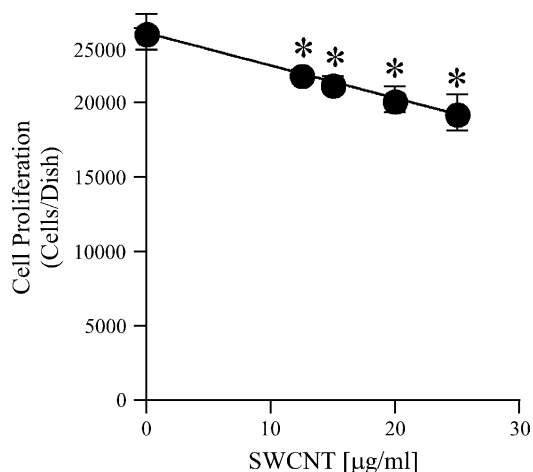
FIG. 6. Effect of SWCNTs on RAW 264.7 macrophage cell number. RAW 264.7 cells were treated with 12.5–30 µg/ml SWCNTs resuspended in normal growth medium by sonication as described in ''Materials and Methods'' section. Cell number was determined using a Coulter Counter 24 h after exposure. Similar results were observed in three separate experiments.

Surfactant-Coated SWCNTs Characterized for Loss of Albumin Adsorption also Lose their Anti-Inflammatory Properties

We next determined whether resuspension of SWCNTs in Pluronic F127, which significantly alters the protein-binding profile (see Fig. 4), influenced their anti-inflammatory activity. We also included a comparison with undiluted sonicated medium alone to illustrate the potential for sonicated medium to contribute to the anti-inflammatory response. RAW 264.7 cells were cotreated for 6 h with LPS and SWCNTs (dispersed in Pluronic F127) or with sonicated medium that had not been diluted. SWCNTs dispersed in Pluronic F127 did not inhibit Cox-2 expression induced by LPS (Fig. 5). Under these conditions, undiluted sonicated medium alone reduced but did
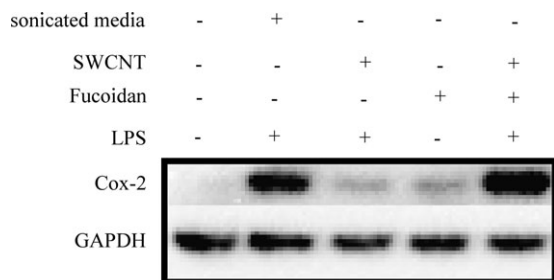

FIG. 7. Inhibition of LPS-mediated Cox-2 expression by SWCNTs. RAW 264.7 cells were treated with 1 ng/ml LPS for 6 h with or without cotreatment with 10 µg/ml SWCNTs (nominal medium concentration; resuspended in normal growth medium by sonication as described in ''Materials and Methods'' section). Some groups were pretreated for 30 min with fucoidan (25 µg/ml) to determine the role of scavenger receptors in this process. Cell lysates were prepared and subjected to Western blot analysis for Cox-2 and GAPDH as described in ''Materials and Methods'' section. Similar results were observed in three separate experiments.

not fully inhibit Cox-2 expression induced by LPS (Fig. 8). In this regard, sonicated medium should be included as a control in all experiments at an equal volume used to deliver nanomaterials and is subject to the same limitations applied to other solvents used in this capacity. For example, solvents (e.g., dimethyl sulfoxide, ethanol, and methanol) have little or no effects when the final concentration is $\leq 0.1\%$. When sonicated medium is diluted 1:100, we do not detect anti-inflammatory activity associated with the medium alone (the induction of Cox-2 by LPS + sonicated medium illustrated in Fig. 7 is not different from Cox-2 induction by LPS alone; data not shown).

Evidence for Scavenger Receptor–Dependent Uptake of SWCNTs

We synthesized a fluor-labeled $SWCNT_{Alexa647}$ to further investigate fucoidan-sensitive uptake. RAW 264.7 cells were treated with $SWCNT_{Alexa647}$ (dispersed in FBS by sonication) with or without a 30-min pretreatment with 25-µg/ml fucoidan. Focal staining pattern of $SWCNT_{Alexa647}$ was observed that was significantly reduced by fucoidan (Fig. 9). This
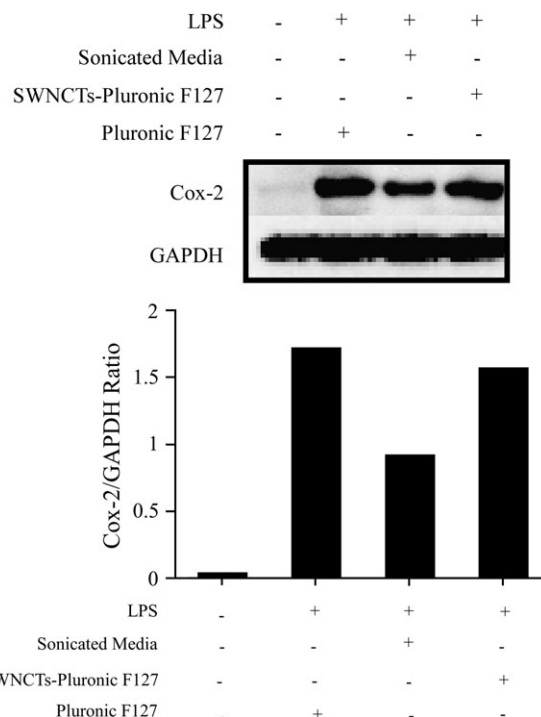

FIG. 8. Resuspension of SWCNTs in emulsifying agent inhibits anti-inflammatory properties. RAW 264.7 cells were treated with 1 ng/ml LPS in the presence or absence of SWCNTs (10 µg/ml) that were resuspended in Pluronic F127 by sonication and subsequently incubated with FBS (10% final) for 60 min. Undiluted sonicated medium was also examined as cotreatment to determine whether damage to medium by sonication could potentially contribute to anti-inflammatory effects in this model. Cell lysates were prepared and subjected to Western blot analysis for Cox-2 and GAPDH as described in ''Materials and Methods'' section. Similar results were observed in three separate experiments.
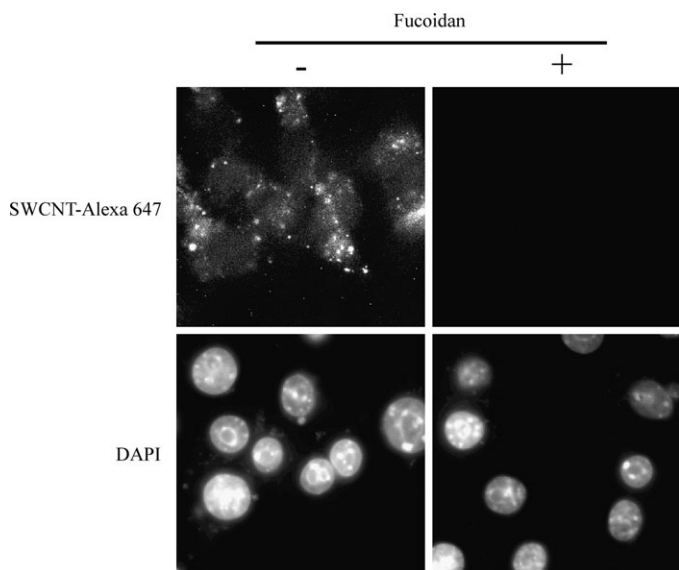
FIG. 9. Inhibition of SWCNT$_{Alexa647}$ uptake by fucoidan. RAW 264.7 cells were treated with 10 μg/ml SWCNT$_{Alexa647}$ for 30 min with or without pretreatment with 25 μg/ml fucoidan for 30 min and SWCNT$_{Alexa647}$ localization determined in fixed cells by epifluorescence microscopy.

observation is consistent with the inhibition of SWCNT anti-inflammatory properties by fucoidan (Fig. 7).

Anti-Inflammatory Effects of SWCNTs Opsinized with Albumin

SWCNTs were resuspended in serum-free medium supplemented with 5% BSA by sonication to determine whether albumin-coated SWCNTs also exhibited anti-inflammatory properties. RAW 264.7 cells were pretreated with albumin-coated SWCNTs (estimated at 8–33 μg/ml; see "Materials and Methods" section) or sonicated medium supplemented with 5% BSA for 30 min, subsequently treated with 1 ng/ml LPS for 6 h, and the semiquantitative Cox-2 and actin levels were determined by Western blot analysis as described in "Materials and Methods" section. Cox-2 levels were significantly increased by LPS, and this response was reduced in a dose-dependent manner by SWCNTs coated with albumin (Fig. 10). This observation is consistent with a role for albumin in the anti-inflammatory response to SWCNTs.

SWCNTs do not Appear to Modulate LPS Binding to RAW 264.7 Macrophage Cells

A fluorescent endotoxin (LPS$_{Alexa488}$; InVitrogen) was used to determine whether SWCNTs interfered with binding of LPS to cells. Western blot analysis indicated that iNOS expression induced by LPS and LPS$_{Alexa488}$ were comparable, indicating that the fluorescent dye does not interfere with the biological properties of LPS$_{Alexa488}$ (Fig. 11, top panel). LPS$_{Alexa488}$ treatment resulted in a plasma membrane and focal staining

pattern (Fig. 11, middle panel). Pretreatment of cells with SWCNTs (dispersed in FBS) did not modulate cell-associated LPS$_{Alexa488}$ fluorescence levels or the qualitative staining pattern (Fig. 11, middle and bottom panels). These data suggest that SWCNTs do not interfere with the binding of LPS to RAW 264.7 cells.

Identification of Proteins Adsorbed to Amorphous Silica with and without Nonionic Surfactant Coating

Similar studies were conducted using a structurally distinct class of nanomaterials (amorphous silica). We examined protein adsorption profiles for amorphous silica ranging from 50 to 1000 nm in size when resuspended in FBS by sonication or when resuspended in Pluronic F127 followed by incubation with FBS for 60 min, and our results are summarized in Figure 12. A number of FBS proteins were observed to adsorb onto amorphous silica and resuspension of silica in Pluronic F127 prior to incubation with FBS-inhibited protein binding (Fig. 12, left panel, results illustrated are for 1000 nm silica). The protein adsorption profile for 50- to 1000-nm silica was comparable (Fig. 12, right panel). In contrast to SWCNTs, albumin was not observed to be the most abundant protein adsorbed onto amorphous silica, indicating that the intrinsic surface property of nanomaterials dictates protein adsorption profiles.

Coating Amorphous Silica with a Nonionic Surfactant Inhibits Cytotoxicity

To further investigate whether dispersing nanomaterials in surfactant modulated the toxic response, we determined cell viability in RAW 264.7 cells treated with 10-nm amorphous silica resuspended in either FBS or Pluronic F127. Treatment of RAW 264.7 cells with 0.78–1.66 μg/ml 10-nm amorphous silica (resuspended in FBS) for 24 h resulted in a dose-dependent decrease in cell number, determined using a Coulter Counter (Fig. 13) and confirmed using an alamar blue cytotoxicity assay (data not shown). Resuspension of 10-nm amorphous silica in Pluronic F127 prior to incubation with FBS fully prevented the decrease in cell number induced by 10-nm amorphous silica. Collectively, our data suggest an important role for adsorbed proteins in guiding the toxicity of nanomaterials with discrete physicochemical properties.

DISCUSSION

We have investigated whether resuspension methods that alter protein adsorption profiles modulate nanomaterial toxicity and whether identification of proteins adsorbed to nanomaterials provides insight into pathway-specific effects. For both SWCNTs and 10-nm amorphous silica, resuspension in an emulsifying agent (Pluronic F127) dramatically reduced protein adsorption and toxicity. In the context of SWCNTs, albumin was identified as the most abundant adsorbed protein
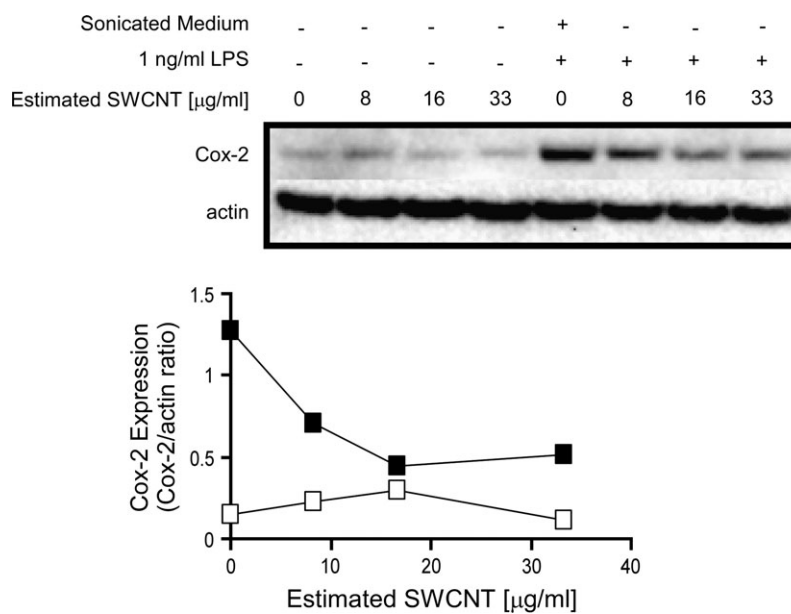
FIG. 10. Inhibition of LPS-mediated Cox-2 induction by albumin-coated SWCNTs. RAW 264.7 cells were pretreated with albumin-coated SWCNTs for 30 min followed by treatment with 1 ng/ml LPS for 6 h. Cox-2 and actin levels were determined by Western blot analysis and quantified using a LumiImager (Roche Diagnostics, Mannheim, Germany). The effects of increasing SWCNT concentration on basal (open) or LPS-induced (solid) Cox-2 levels are illustrated. Similar results were observed in two separate experiments.

from FBS and human serum/plasma but not when plasma from the albumin-deficient NAR was used. Damaged or structurally altered albumin is a well-known ligand for scavenger receptors, and the uptake (Fig. 9) and anti-inflammatory effects of SWCNTs (Fig. 7) were inhibited by fucoidan, a scavenger receptor antagonist. Coating SWCNTs with albumin alone was sufficient to reduce Cox-2 induction by LPS (Fig. 10). These observations are consistent with the observation that albumin is the major protein adsorbed onto SWCNTs and the known targeting of albumin to scavenger receptors. Thus, our data indicate that identification of the proteins adsorbed onto nanomaterials *a priori* may provide important information regarding pathway-specific uptake, which in turn has logical implications for predicting disposition.

Due to their small size, nanomaterials are expected to gain access to sites within cells and tissues that have not previously or routinely been encountered, which in combination with unique physicochemical properties raises concern that new modes of toxicity may arise. Methods to predict nanomaterial disposition are needed to reduce these uncertainties. There is a long history describing a decisive role for adsorbed proteins (e.g., opsonins) in regulating toxicant disposition that is relevant to nanomaterials and can be exploited to improve toxicity assessment. In this regard, we believe that the identification of albumin as the most abundant protein adsorbed onto SWCNTs (Figs. 4 and 5) is highly consistent with *in vivo* disposition profiles associated with carbonaceous nanomaterials. Specifically, 73–80% of fullerenes administered iv are retained in the liver for at least 7 days (Yamago *et al.,* 1995). Similarly, 24 h

after iv administration, significant concentrations of SWCNTs are only observed in the liver (Cherukuri *et al.,* 2006). Carbonaceous nanomaterials including fullerenes and SWCNTs are known to complex with albumin (Belgorodsky *et al.,* 2006; Matsuura *et al.,* 2006), and our data suggest that the levels of albumin adsorbed onto SWCNTs far exceed the levels associated with the second most abundant protein (Figs. 4 and 5), affording albumin-targeted pathways a competitive advantage. Damaged or structurally altered albumin is rapidly cleared from circulation by scavenger receptors, and in fact, damaged albumin is frequently used to establish a role for scavenger receptors in experimental model systems. Specific examples include maleylated albumin (Demoy *et al.,* 1999), formaldehyde-treated albumin (Jansen *et al.,* 1991), albumin derivatized with *cis*-aconitic anhydride (Kamps *et al.,* 1997), and others (Hamblin *et al.,* 2000; Hansen *et al.,* 2002; Tokuda *et al.,* 1993). In studies examining maleylated albumin interaction with scavenger receptor, it was concluded that alterations in the primary sequence of albumin, rather than addition of new negative charge, provides the recognition determinant essential for interaction with the scavenger receptor (Haberland and Fogelman, 1985). Precision cut organ slices also support a role for albumin in directing scavenger receptor–dependent uptake of nanomaterials. Specifically, nanoparticle capture using precision cut spleen slices was not decreased when complement, immunoglobulins or heparin-binding proteins were depleted from the medium, while substitution of serum by purified albumin allowed a near optimal uptake in a scavenger receptor–dependent fashion (Demoy *et al.,* 1999). When albumin is used
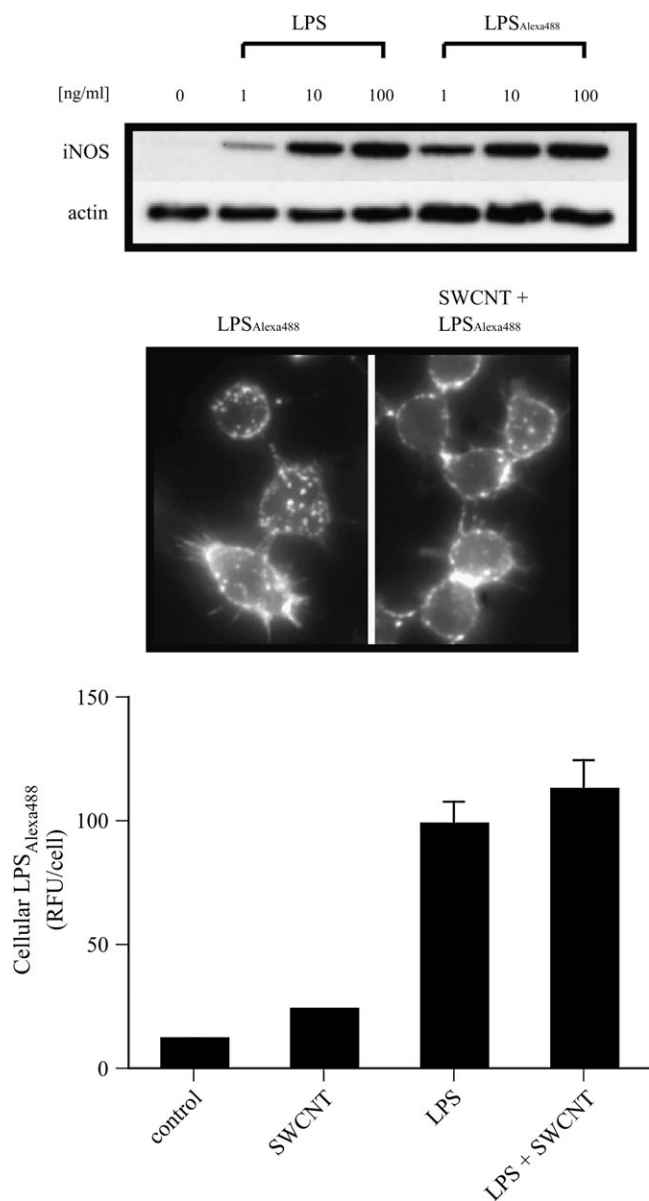
FIG. 11. SWCNTs do not reduce cell-associated LPS$_{Alexa488}$ fluorescence in RAW 264.7 cells. RAW 264.7 cells were treated with 1–100 ng/ml LPS or LPS$_{Alexa488}$ for 6 h, and iNOS induction was determined by Western blot analysis (top). Cellular LPS$_{Alexa488}$ staining pattern was determined with and without cotreatment with SWCNTs (middle) and quantified using Metamorph Software (bottom). Similar results were observed in two separate experiments.

as a drug carrier, minimal loading rates (approximately 1 mole of drug per mole of albumin) are required for optimal targeting properties, while higher drug loading rates (> 1 mol drug per mol albumin) frequently result in efficient uptake of the albumin-drug complex by scavenger receptors in liver (Hamblin *et al.,* 2000; Stehle *et al.,* 1997). Collectively, these observations suggest that only minor modification to albumin structure, as could occur upon binding to carbonaceous nanomaterials, may result in recognition of albumin as
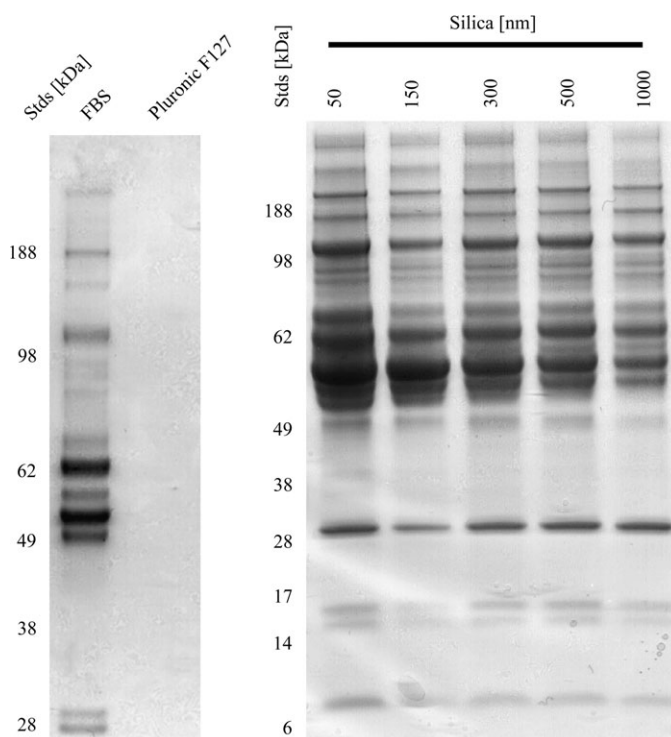

FIG. 12. Qualitative FBS protein adsorption profile associated with amorphous silica (50–1000 nm) with or without Pluronic F127 coating. Silica was resuspended in normal growth medium by sonication or Pluronic F127 by sonication followed by incubation with FBS (10% final) for 60 min as described in ''Materials and Methods'' section. Silica was then washed three times with PBS, and proteins were desorbed and analyzed by SDS-PAGE. Similar results were observed in five separate experiments.

a damaged form by scavenger receptors. Hepatic scavenger receptors are exquisitely efficient in clearing damaged albumin from circulation (Kamps *et al.,* 1997; Mukhopadhyay *et al.,* 1995), therefore, this pathway could contribute to hematological surveillance and maintenance in a manner that would
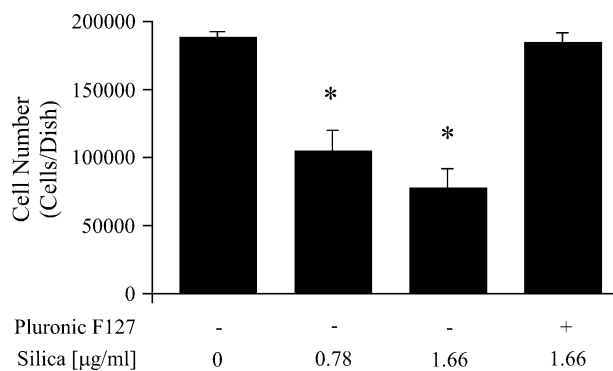

FIG. 13. Resuspension of 10-nm amorphous silica in Pluronic F127 inhibits toxicity. RAW 264.7 cells were treated with 0.78–1.66 μg/ml, 10-nm amorphous silica for 18 h with or without resuspension in Pluronic F127 followed by incubation with FBS (10% final) for 60 min. Values represent the mean ± SE. *Significantly different from control, $p < 0.05$. Similar results were observed in two separate experiments.

significantly affect clearance of nanoparticles from blood and uptake into tissues.

We observe that SWCNTs antagonize the inflammatory response to bacterial endotoxin in the RAW 264.7 macrophage–like cell line (see Fig. 7). Macrophages represent a primary line of defense and generate reactive nitrogen and oxygen species as well as a host of inflammatory cytokines (e.g., tumor necrosis factor α) that facilitate the killing of pathogens and cancer cells (Accolla, 2006; Klimp et al., 2002). Cox-2 and iNOS are important mediators of inflammatory responses induced by endotoxin (Chen et al., 2006; Weber et al., 2006). The significance of our findings have not yet been fully established; however, these observations suggest that targeting of the scavenger receptor pathway by a SWCNT-albumin complex could result in interference with the innate immune response. There are a number of published works providing precedence for the scavenger receptor–dependent anti-inflammatory effects observed here. Specifically, scavenger receptor activation is associated with the inhibition of important inflammatory mediators (e.g., iNOS) by endotoxin (Matsuno et al., 1997). Lack of effect of lysosomotropic agents on this response suggest that binding of scavenger receptor ligand (maleylated albumin) to scavenger receptor generates a signal that is involved in the inhibition of the induction of inflammatory mediators by LPS. Independent investigators have observed that class A scavenger receptors counter the activities of proinflammatory receptors and attenuate the production of specific chemokines to ensure an inflammatory response of the appropriate magnitude (Cotena et al., 2004). Endotoxin may be internalized by several pathways including scavenger receptors; however, binding and internalization of endotoxin has been associated with class B type I scavenger receptors which represent a distinct binding site for endotoxin, relative to the anti-inflammatory class A scavenger receptors (Vishnyakova et al., 2003). RAW 264.7 macrophage–like cells have been used in our studies, and in vitro competition studies conducted in RAW 264.7 cells indicate that scavenger receptor binding is not involved in LPS-mediated activation (Hampton et al., 1991), consistent with our data indicating that SWCNT-albumin complex targets a scavenger receptor but does not interfere with LPS$_{Alexa488}$ binding to RAW 264.7 cells (Figs. 7 and 11). RAW 264.7 cells express class A scavenger receptors (Coller and Paulnock, 2001; Daugherty et al., 2000) providing a plausible link between relevant scavenger receptor expression in this model, the observed scavenger receptor targeting of a SWCNT-albumin complex, and the inhibition of endotoxin-mediated Cox-2 expression by SWCNTs.

The impetus for nanotoxicology is to proactively define toxic modes of action that could potentially arise in occupational, environmental, or medical settings. One of the major challenges in this regard is the accurate quantification of nanomaterial dose and translation to real-world exposure scenarios. The present studies are limited by accuracy of the estimates of dosimetry, which is influenced by many factors including particle agglomeration and settling (Teeguarden et al., 2007) and represent the cellular response to SWCNTs in relation to estimated nominal medium concentrations. Additional factors that could complicate the prediction of nanomaterial disposition as directed by adsorbed proteins include the route of exposure and compartmental regulation. While serum proteins have been used here as a convenient test case that may be relevant to nanomaterials reaching systemic circulation (as could occur with medical applications), they may not adequately reflect the proteins that may come into first contact with nanomaterials by other routes of exposure. In addition, questions remain regarding the displacement of proteins and relative protein stoichiometries that may arise when a nanomaterial reaches systemic circulation from pulmonary, gastrointestinal, or dermal routes of exposure, as well as the proteins that may be associated with the redistribution of nanomaterials that can occur subsequent to acute disposition profiles (Takenaka et al., 2001). Despite these challenges, our data suggest that modulation of the immune response should be one mode of action to consider when investigating or monitoring potential adverse health effects associated with carbonaceous nanomaterials.

Albumin was consistently identified as the most abundant protein adsorbed to SWCNTs following incubation with FBS or human plasma/serum (Figs. 4 and 5). When albumin-deficient NAR plasma was used, albumin adsorption to SWCNTs was not detected and a markedly different protein adsorption profile was observed (Fig. 5). Albumin was not the most abundant protein adsorbed to amorphous silica (note that several bands appear comparable in Fig. 12), suggesting that the intrinsic surface properties of nanomaterials will dictate protein adsorption profiles. Thus, carbonaceous nanomaterials appear to have a high affinity for albumin in the absence of surface modifications. In the case of silica, we did not observe that size dramatically influenced the qualitative protein adsorption profile (Fig. 12). This latter observation raises the possibility that nanomaterials could be used in convenient larger bulk sizes, providing that the surface chemistry is the same, to define adsorbed protein stoichiometry for consideration in toxicity assessment and disposition of the corresponding nano-sized forms. In the present studies, we used plasma and serum to investigate potential contributions of hematological components in guiding disposition. An obvious extension of this work would include appropriate tissue extracts to capture protein-binding profiles associated with the route of exposure under investigation.

The use of a surfactant (e.g., Pluronic F127) to disperse SWCNTs and amorphous silica results is a dramatic loss of protein binding and toxicity (Figs. 8 and 13). Thus, while surfactants may conveniently disperse and prevent aggregation of nanomaterials, they could also prevent the formation of important protein-nanomaterial complexes that govern uptake and disposition, which in turn can be important determinants of toxicity. Alternatively, in cases where the surfactant coating

results in a qualitative shift in protein adsorption profiles (see apparent shift to casein-related proteins adsorbed to Pluronic F127–coated SWCNTs; Fig. 4), the use of surfactants could potentially result in uptake of nanomaterials by pathways associated with the proteins that are specifically adsorbed to their surfactant-coated surface, which may not reflect disposition in the absence of surfactant. In addition, some surfactants are reported to allow the material under investigation to be physisorbed by lipids and proteins from the local microenvironment. It is reasonable to hypothesize that the relative stoichiometry of proteins adsorbed to nanomaterial surfaces will competitively influence pathway-specific uptake. Thus, if a surfactant qualitatively or quantitatively alters protein adsorption profiles, there is a potential for skewing of the uptake pathway and associated mode of action *in vitro*. Although not specifically investigated here, it is also important to recognize that affinity of adsorbed proteins for their respective cognizant receptors and kinetics of uptake may also be important determinants of disposition *in vivo*. Thus, it is prudent to evaluate the relative contribution of adsorbed proteins in guiding nanomaterial disposition and toxicity, and careful attention to these components *in vitro* may improve extrapolation of results to more complex models and humans.

REFERENCES

Accolla, R. S. (2006). Host defense mechanisms against pathogens. *Surg. Infect. (Larchmt)* **7**(Suppl. 2), S5–S7.

Belgorodsky, B., Fadeev, L., Kolsenik, J., and Gozin, M. (2006). Formation of a soluble stable complex between pristine C60-fullerene and a native blood protein. *Chembiochem* **7**, 1783–1789.

Chen, C. H., Sheu, M. T., Chen, T. F., Wang, Y. C., Hou, W. C., Liu, D. Z., Chung, T. C., and Liang, Y. C. (2006). Suppression of endotoxin-induced proinflammatory responses by citrus pectin through blocking LPS signaling pathways. *Biochem. Pharmacol.* **72**, 1001–1009.

Cherukuri, P., Gannon, C. J., Leeuw, T. K., Schmidt, H. K., Smalley, R. E., Curley, S. A., and Weisman, R. B. (2006). Mammalian pharmacokinetics of carbon nanotubes using intrinsic near-infrared fluorescence. *Proc. Natl. Acad. Sci. USA* **103**, 18882–18886.

Coller, S. P., and Paulnock, D. M. (2001). Signaling pathways initiated in macrophages after engagement of type A scavenger receptors. *J. Leukoc. Biol.* **70**, 142–148.

Cotena, A., Gordon, S., and Platt, N. (2004). The class A macrophage scavenger receptor attenuates CXC chemokine production and the early infiltration of neutrophils in sterile peritonitis. *J. Immunol.* **173**, 6427–6432.

Daugherty, A., Whitman, S. C., Block, A. E., and Rateri, D. L. (2000). Polymorphism of class A scavenger receptors in C57BL/6 mice. *J. Lipid Res.* **41**, 1568–1577.

Demoy, M., Andreux, J. P., Weingarten, C., Gouritin, B., Guilloux, V., and Couvreur, P. (1999). In vitro evaluation of nanoparticles spleen capture. *Life Sci.* **64**, 1329–1337.

Douglas, S. J., Davis, S. S., and Illum, L. (1987). Nanoparticles in drug delivery. *Crit. Rev. Ther. Drug Carrier Syst.* **3**, 233–261.

Geiser, M., Rothen-Rutishauser, B., Kapp, N., Schurch, S., Kreyling, W., Schulz, H., Semmler, M., Im Hof, V., Heyder, J., and Gehr, P. (2005). Ultrafine particles cross cellular membranes by nonphagocytic mechanisms in lungs and in cultured cells. *Environ. Health Perspect.* **113**, 1555–1560.

Goppert, T. M., and Muller, R. H. (2005). Polysorbate-stabilized solid lipid nanoparticles as colloidal carriers for intravenous targeting of drugs to the brain: Comparison of plasma protein adsorption patterns. *J. Drug Target* **13**, 179–187.

Haberland, M. E., and Fogelman, A. M. (1985). Scavenger receptor-mediated recognition of maleyl bovine plasma albumin and the demaleylated protein in human monocyte macrophages. *Proc. Natl. Acad. Sci. USA* **82**, 2693–2697.

Hamblin, M. R., Miller, J. L., and Ortel, B. (2000). Scavenger-receptor targeted photodynamic therapy. *Photochem. Photobiol.* **72**, 533–540.

Hampton, R. Y., Golenbock, D. T., Penman, M., Krieger, M., and Raetz, C. R. (1991). Recognition and plasma clearance of endotoxin by scavenger receptors. *Nature* **352**, 342–344.

Hansen, B., Svistounov, D., Olsen, R., Nagai, R., Horiuchi, S., and Smedsrod, B. (2002). Advanced glycation end products impair the scavenger function of rat hepatic sinusoidal endothelial cells. *Diabetologia* **45**, 1379–1388.

Hermanson, G. (1996). *Bioconjugate Techniques*. Academic Press, San Diego, CA.

Jansen, R. W., Molema, G., Harms, G., Kruijt, J. K., van Berkel, T. J., Hardonk, M. J., and Meijer, D. K. (1991). Formaldehyde treated albumin contains monomeric and polymeric forms that are differently cleared by endothelial and Kupffer cells of the liver: Evidence for scavenger receptor heterogeneity. *Biochem. Biophys. Res. Commun.* **180**, 23–32.

Kamps, J. A., Morselt, H. W., Swart, P. J., Meijer, D. K., and Scherphof, G. L. (1997). Massive targeting of liposomes, surface-modified with anionized albumins, to hepatic endothelial cells. *Proc. Natl. Acad. Sci. USA* **94**, 11681–11685.

Klimp, A. H., de Vries, E. G., Scherphof, G. L., and Daemen, T. (2002). A potential role of macrophage activation in the treatment of cancer. *Crit. Rev. Oncol. Hematol.* **44**, 143–161.

Krieger, M., and Herz, J. (1994). Structures and functions of multiligand lipoprotein receptors: Macrophage scavenger receptors and LDL receptor-related protein (LRP). *Ann. Rev. Biochem.* **63**, 601–637.

Matsuno, R., Aramaki, Y., Arima, H., and Tsuchiya, S. (1997). Scavenger receptors may regulate nitric oxide production from macrophages stimulated by LPS. *Biochem. Biophys. Res. Commun.* **237**, 601–605.

Matsuura, K., Saito, T., Okazaki, T., Oshshima, S., Yumura, M., and Iijima, S. (2006). Selectivity of water-soluble proteins in single-walled carbon nanotube dispersions. *Chem. Phys. Lett.* **429**, 497–502.

Mercer, R. R., Scabilloni, J. F., Wang, L., Schwegler-Berry, D., Shvedova, A. A., and Castranova, V. (2007). Dispersion significantly enhances the pulmonary toxicity of single walled carbon nanotubes. In Society of Toxicology, Vol. Abstract 46th Annual Meeting. p. 1115, Oxford University Press, Charlotte, NC.

Moghimi, S. M., Muir, I. S., Illum, L., Davis, S. S., and Kolb-Bachofen, V. (1993). Coating particles with a block co-polymer (poloxamine-908) suppresses opsonization but permits the activity of dysopsonins in the serum. *Biochim. Biophys. Acta* **1179,** 157–165.

Mukhopadhyay, A., Mukhopadhyay, B., and Basu, S. K. (1995). Circumvention of multidrug resistance in neoplastic cells through scavenger receptor mediated drug delivery. *FEBS Lett.* **376,** 95–98.

Nel, A., Xia, T., Madler, L., and Li, N. (2006). Toxic potential of materials at the nanolevel. *Science* **311,** 622–627.

Oberdorster, G., Oberdorster, E., and Oberdorster, J. (2005). Nanotoxicology: An emerging discipline evolving from studies of ultrafine particles. *Environ. Health Perspect.* **113,** 823–839.

Qian, W. J., Liu, T., Monroe, M. E., Strittmatter, E. F., Jacobs, J. M., Kangas, L. J., Petritis, K., Camp, D. G., III, and Smith, R. D. (2005). Probability-based evaluation of peptide and protein identifications from tandem mass spectrometry and SEQUEST analysis: The human proteome. *J. Proteome Res.* **4,** 53–62.

Shen, Y., Zhao, R., Belov, M. E., Conrads, T. P., Anderson, G. A., Tang, K., Pasa-Tolic, L., Veenstra, T. D., Lipton, M. S., Udseth, H. R., *et al.* (2001). Packed capillary reversed-phase liquid chromatography with high-performance electrospray ionization Fourier transform ion cyclotron resonance mass spectrometry for proteomics. *Anal. Chem.* **73,** 1766–1775.

Stehle, G., Sinn, H., Wunder, A., Schrenk, H. H., Schutt, S., Maier-Borst, W., and Heene, D. L. (1997). The loading rate determines tumor targeting properties of methotrexate-albumin conjugates in rats. *Anticancer Drugs* **8,** 677–685.

Takenaka, S., Karg, E., Roth, C., Schulz, H., Ziesenis, A., Heinzmann, U., Schramel, P., and Heyder, J. (2001). Pulmonary and systemic distribution of inhaled ultrafine silver particles in rats. *Environ. Health Perspect.* **109** (Suppl. 4), 547–551.

Teeguarden, J. G., Hinderliter, P. M., Orr, G., Thrall, B. D., and Pounds, J. G. (2007). Particokinetics in vitro: Dosimetry considerations for in vitro nanoparticle toxicity assessments. *Toxicol. Sci.* **95,** 300–312.

Tokuda, H., Masuda, S., Takakura, Y., Sezaki, H., and Hashida, M. (1993). Specific uptake of succinylated proteins via a scavenger receptor-mediated mechanism in cultured brain microvessel endothelial cells. *Biochem. Biophys. Res. Commun.* **196,** 18–24.

Vishnyakova, T. G., Bocharov, A. V., Baranova, I. N., Chen, Z., Remaley, A. T., Csako, G., Eggerman, T. L., and Patterson, A. P. (2003). Binding and internalization of lipopolysaccharide by Cla-1, a human orthologue of rodent scavenger receptor B1. *J. Biol. Chem.* **278,** 22771–22780.

Weber, T. J., Smallwood, H. S., Kathmann, L. E., Markillie, L. M., Squier, T. C., and Thrall, B. D. (2006). Functional linkage between tumor necrosis factor biosynthesis and calmodulin-dependent activation of iNOS in RAW 264.7 macrophages. *Am. J. Physiol. Cell Physiol.* **290,** C1512–C1520.

Yamago, S., Tokuyama, H., Nakamura, E., Kikuchi, K., Kananishi, S., Sueki, K., Nakahara, H., Enomoto, S., and Ambe, F. (1995). In vivo biological behavior of a water-miscible fullerene: 14C labeling, absorption, distribution, excretion and acute toxicity. *Chem. Biol.* **2,** 385–389.

Zhao, W., Song, C., and Pehrsson, P. E. (2002). Water-soluble and optically pH-sensitive single-walled carbon nanotubes from surface modification. *J. Am. Chem. Soc.* **124,** 12418–12419.